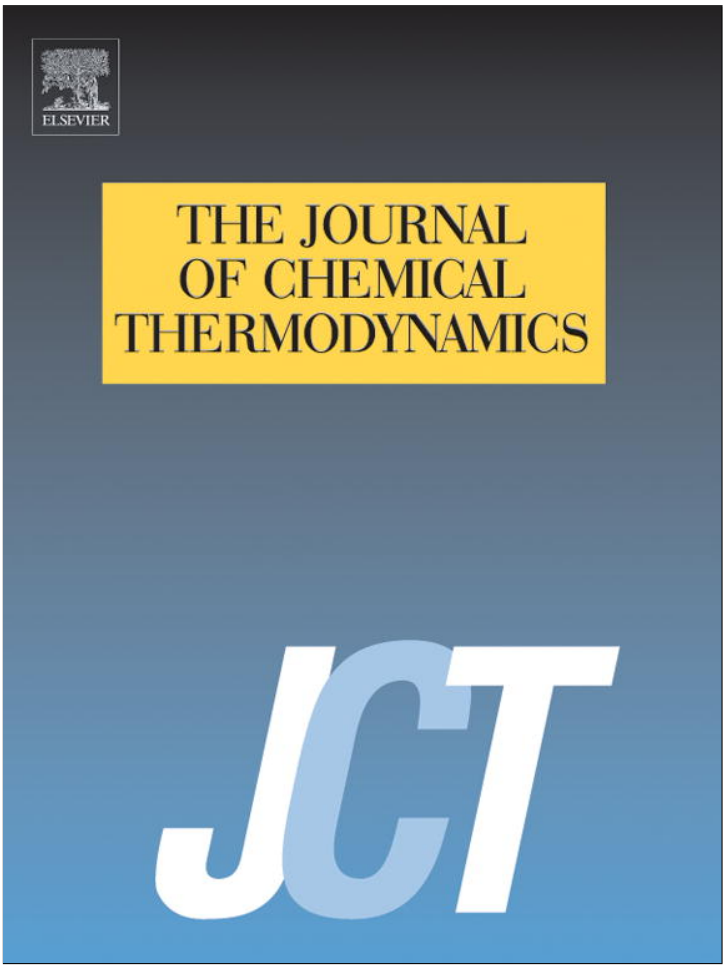

(This is a sample cover image for this issue. The actual cover is not yet available at this time.)

J. Chem. Thermodynamics 58 (2013) 206–210

Contents lists available at SciVerse ScienceDirect

J. Chem. Thermodynamics

journal homepage: www.elsevier.com/locate/jct

Application of molecular modelling and spectroscopic approaches for investigating the binding of tanshinone IIA to human serum albumin

Jinhua Li *, Sumin Wang

School of Materials and Chemical Engineering, Xi'an Technological University, Xi'an 710032, China

ARTICLE INFO

Article history:
Received 1 October 2012
Received in revised form 4 November 2012
Accepted 5 November 2012
Available online 23 November 2012

Keywords:
Molecular modelling
Tanshinone IIA
Human serum albumin
Fluorescence quenching technology
FT-IR spectroscopy
Circular dichroism

ABSTRACT

The interaction of tanshinone IIA and human serum albumin (HSA) has been characterised by molecular modelling, fluorescence, Fourier transform infrared (FT-IR) and circular dichroism (CD) spectroscopic methods. The results of molecular modelling suggested that tanshinone IIA located within the binding pocket of subdomain IIA of HSA is held mainly by hydrophobic forces. Fluorescence titration revealed that tanshinone IIA could quench the intrinsic fluorescence of HSA. The binding constants at three temperatures (296, 303, and 310) K are ($6.42 \cdot 10^4$, $1.54 \cdot 10^5$, and $4.35 \cdot 10^5$) $dm^3 \cdot mol^{-1}$, respectively. In addition, the studies of CD spectroscopy and FT-IR spectroscopy showed that the binding of tanshinone IIA to HSA changed molecular conformation of HSA.

1. Introduction

Tanshinone IIA (structure shown in figure 1), a derivative of phenanthrenequinone, is the major component isolated from *Salvia miltiorrhiza* (Danshen, in Chinese) which is a well-known traditional Chinese herbal medicine. It has been reported to display a great variety of pharmacological activities including prevention of angina pectoris and myocardial infarction [1], anticancer [2,3], and antioxidant [4] properties. Moreover, recent research indicates that tanshinone IIA may possess complex inhibiting and inducting action on CYP1A [5].

Human serum albumin (HSA), the most abundant carrier protein in blood circulation, plays a major role in the transport and deposition of many endogenous and exogenous drugs ligands in blood [6,7]. A number of the relatively insoluble endogenous compounds and a wide variety of drugs can bind to albumin and other serum components, which implicates HSA's role as a carrier [8,9]. Due to the availability of hydrophobic pockets inside the protein network and the flexibility of the albumins to adapt its shape [10], serum albumin can increase the apparent solubility of hydrophobic drugs in plasma and modulates their delivery to cells *in vivo* and *in vitro*. Therefore, investigating the binding of the drug to HSA can provide useful information of structural features that determine the therapeutic effectiveness of drugs. Binding studies have become an important research field in life sciences, chemistry and clinical medicine. There are some works [11–13] underway to study the interaction of the drug with protein by the fluorescence technique, Fourier transform infrared spectroscopy (FT-IR), circular dichroism (CD) spectroscopy, and molecular modelling. However, none of the investigations determines in detail the tanshinone IIA–HSA binding constants and the effect of tanshinone IIA complexation on the protein structure.

In this paper, molecular modelling and multi-spectroscopic methods were employed to demonstrate the interaction of tanshinone IIA–HSA. First, the molecular docking was performed to reveal binding tanshinone IIA to HSA through SGI FUEL workstations (theoretical model). Then, thermodynamic data of binding (including binding mechanism, binding constant) of tanshinone IIA to HSA were studied under simulative physiological conditions utilising the fluorescence method. The effect of tanshinone IIA on the structure of HSA was also examined using Fourier transform infrared spectroscopy and circular dichroism spectroscopy.

2. Materials and methods

2.1. Materials

Human serum albumin (HSA) was purchased from Sigma Chemical Company. All HSA solutions were prepared in pH 7.40 buffer solution, and HSA stock solution was kept in the dark at $T = 277$ K. Tanshinone IIA (analytical grade) was obtained from the National Institute for Control of Pharmaceutical and

* Corresponding author. Tel.: +86 29 88491834; fax: +86 29 89491716.
E-mail address: lijhua09@163.com (J. Li).

0021-9614/$ - see front matter © 2012 Elsevier Ltd. All rights reserved.
http://dx.doi.org/10.1016/j.jct.2012.11.009

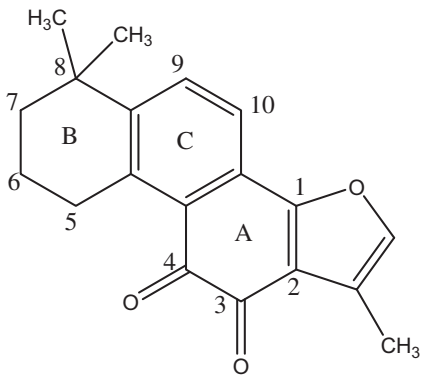

FIGURE 1. The chemical structure of tanshinone IIA.

Bioproducts, China. The stock solution ($1.0 \cdot 10^{-4}$ mol · dm^{-3}) was prepared in ethanol. NaCl (analytical grade, 1.0 mol · dm^{-3}) solution was used to maintain the ion strength at 0.1. The buffer (pH 7.40) consists of tris (0.2 mol · dm^{-3}) and HCl (0.1 mol · dm^{-3}). The pH was checked with a suitably standardized pH meter. All reagents were of analytical reagent grade and distilled water was used throughout the experiment.

2.2. Apparatus and methods

Molecular modelling was investigated through SGI FUEL WORKSTATION. The crystal structure of HSA in complex with R-Warfarin was taken from the Brookhaven Protein Data Bank (entry codes 1 h9z) [14]. The potential of the 3-D structure of HSA was assigned according to the Amber 4.0 force field with Kollman-all-atom charges. The initial structures of all the molecules were generated by molecular modelling soft-ware SYBYL 6.9 [15]. The geometries of these compounds were subsequently optimised using the Tripos force field with Gasteiger-Marsili charges. The FlexX program was applied to calculate the possible conformation of the ligands that bind to the protein.

All the fluorescence spectra were performed on a RF-5301PC Spectrofluorophotometer (Shimadzu, Japan), using 5 nm/5 nm slit widths. The excitation wavelength was 280 nm, and the emission wavelengths were red at (300 to 480) nm.

Fluorescence titration experiments: 3.0 cm^3 solution containing appropriate concentration of HSA was titrated manually by successive addition of a $1.0 \cdot 10^{-4}$ mol · dm^{-3} ethanol stock solution of tanshinone IIA (to give a final concentration of ($3.3 \cdot 10^{-7}$ to $3.0 \cdot 10^{-6}$) mol · dm^{-3}) with trace syringes, and the fluorescence intensity was measured (excitation at 280 nm and emission at 335 nm). All experiments were measured at different temperature (296, 303, and 310) K. The temperature of sample was kept by recycled water throughout the experiment.

The UV absorbance spectra were recorded using a CARY-100 UV–vis spectrometer (Varian, USA) equipped with 1.0 cm quartz cells.

FT-IR measurements were carried out at room temperature on a Nicolet Nexus 670 FT-IR spectrometer (USA) equipped with a Germanium attenuated total reflection (ATR) accessory, a DTGS KBr detector and a KBr beam splitter. All spectra were taken via the attenuated total reflection (ATR) method with a resolution of 4 cm^{-1} and 60 scans. The infrared spectra of HSA and tanshinone IIA–HSA complex (the molar ratio of tanshinone IIA to HSA was 2:1) were obtained in the featured region of (2200 to 1300) cm^{-1}. Corresponding absorbance contributions of buffer and free tanshinone IIA solutions were recorded and subtracted with the same instrumental parameters. The subtraction criterion was that the original spectrum of the protein solution between (2200 and 1800) cm^{-1} was featureless [16,17].

Circular dichroism was made on a Jasco-20 automatic recording spectropolarimeter (Japan), using a 2 mm cell at $T = 296$ K. The spectra were recorded over the range of 200 to 300 nm. The results are expressed as molar ellipticity ($[\theta]$) in deg · cm^2 · dmol^{-1}. The α-helical content of HSA was calculated from the $[\theta]$ value at 208 nm using the equation: $\alpha\%\text{helix} = \{(-[\theta]_{208} - 4000)/(33{,}000 - 4000)\} \cdot 100$ as described by Lu *et al.* [18].

3. Results and discussion

3.1. Molecular modelling study of the interaction between tanshinone IIA and HSA

The application of molecular modelling by the computer method has been employed to predict the interaction of tanshinone IIA and HSA. The crystallographic analyses of HSA have revealed that the protein, a 585 amino acid residues monomer, contains three homologous a-helical domains (I–III): I (residues 1–195), II (residues 196–383), III (residues 384–585), and each containing two subdomains (A and B) [19]. It is reported that HSA has binding sites in sub-domains IIA and IIIA, which are corresponding to site I and site II, respectively, and a single tryptophan residue (Trp-214) is in subdomain IIA [20,21]. There is a large hydrophobic cavity present in sub-domain IIA that many drugs can band at. The best energy ranked result is shown in figure 2. From figure 2, it can be seen that tanshinone IIA binds within the subdomain IIA of the protein (The Warfarin Binding Pocket), and it is important to note that the tryptophan residue of HSA (Trp-214) is in close proximity to B ring of tanshinone IIA, suggesting the existence of hydrophobic interaction between them. Further, the finding provides a good structure basis to explain the efficient fluorescence quenching of HSA emission in the presence of tanshinone IIA. On the other hand, figure 2 shows that the residues Arg-218 and Arg-222 of HSA are suitable to form intermolecular H-bond with 1-O. In addition, Lys-195 is also able to form H-bond with 3-O. The result indicated that the formation of hydrogen bonds decreased the hydrophilicity and increased the hydrophobicity to stability the (tanshinone IIA + HSA) system. Therefore the results obtained from modelling indicate

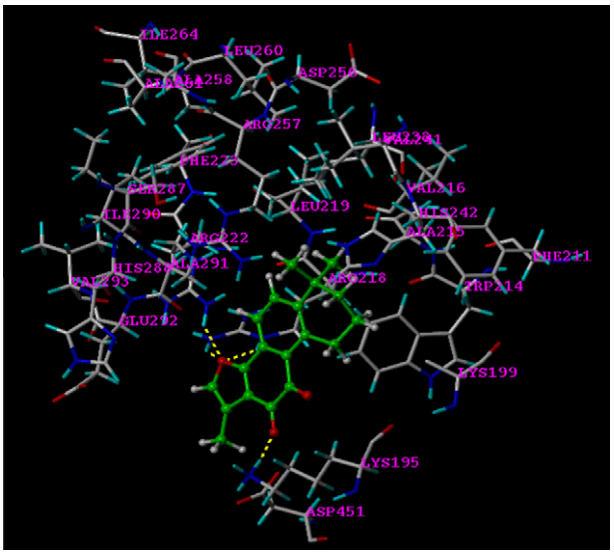

FIGURE 2. The interaction mode between tanshinone IIA and HSA. The residues of HSA are represented using line and tanshinone IIA structure is represented using ball and stick model. The hydrogen bond between tanshinone IIA and HSA is represented using dashed line.

that the interaction between tanshinone IIA and HSA is dominated by hydrophobic force, and there is also hydrogen bond interaction between the drug and the residues of HSA. Some spectral experiments were thus taken to obtain information related to the binding mechanisms and validate the results from molecular modelling.

3.2. The mechanism of fluorescence quenching

The effect of tanshinone IIA on HSA and the conformation changes of HSA were evaluated by measuring the intrinsic fluorescence intensity of protein before and after the addition of tanshinone IIA. Figure 3 shows the fluorescence emission spectra of HSA with the addition of different low concentration of tanshinone IIA (the solubility of tanshinone IIA is very low in water, the higher concentration of tanshinone IIA cannot be obtained). The HSA has a strong fluorescence emission with a peak at 335 nm at λ_{ex} 280 nm, while tanshinone IIA was almost non-fluorescent at λ_{ex} 280 nm. It can be seen that the addition of tanshinone IIA results in a significant reduction in the fluorescence intensity indicating that the binding of tanshinone IIA to HSA quenches the intrinsic fluorescence of the single tryptophan in HSA (Trp-214), which was in agreement with the results obtained by molecular modelling. Meanwhile, a shift of emission to shorter wavelength from (335 to 331) nm was also observed, suggesting the polarity of the protein environment was lower compared to that of the pure protein solution.

Fluorescence quenching may result from a variety of processes such as static quenching, dynamic quenching and non-radiative energy transfer [22]. Static quenching is due to the formation of ground-state complex between the fluorophore and the quencher, dynamic quenching results from collision between them. In general, static and dynamic quenching can be distinguished by their differing dependence on temperature. For static quenching, the quenching constants decrease with increasing temperature, while the quenching constants increase with increasing temperature for dynamic quenching. The fluorescence quenching data are analysed by the Stern–Volmer equation (1) to recognise the quenching mechanism:

$$F_0/F = 1 + K_{SV}[Q] = 1 + K_q\tau_0[Q], \quad (1)$$

where F and F_0 are the relative fluorescence intensities in the presence and absence of quencher, respectively. [Q] is the concentration of quencher, K_{SV} is the Stern–Volmer quenching constant, K_q is the quenching constant of bimolecular fluorescence, τ_0 is the lifetime of the fluorophore in the absence of quencher (HSA: 10^{-8} s), $K_q = K_{SV}/\tau_0$. The possible quenching mechanism can be interpreted by the Stern–Volmer curves. Figure 4 shows the Stern–Volmer quenching plots of tanshinone IIA with HSA at different temperatures (296, 303, and 310) K. There is a linear dependence between F_0/F and [Q] and the slopes increase with increasing temperature (which were ($1.91 \cdot 10^4$, $2.11 \cdot 10^5$, and $2.15 \cdot 10^5$) $dm^3 \cdot mol^{-1}$ at (296, 303, and 310) K) revealing the occurrence of dynamic quenching interaction between tanshinone IIA and HSA [23]. Moreover, the values of K_q were all greater than $2.0 \cdot 10^{10}$ $dm^3 \cdot mol^{-1}\ S^{-1}$ (the maximum diffusion collision quenching rate constant) which indicated that the static quenching may also exist between them [24]. For static quenching, the absorption spectra of fluorescence substance would be changed because of the formation of ground-state complex [25]. Figure 5 shows that the absorption spectra of tanshinone IIA, HSA and tanshinone IIA–HSA were different. The band maxima of the free HSA at 280 nm and the absorbance of HSA increased with the addition of tanshinone IIA. In addition, the position peak of HSA has a blue shift. The reason may be that the peptide strands of protein molecules extended because of the binding of tanshinone IIA to HSA [26]. The evidence from UV spectra

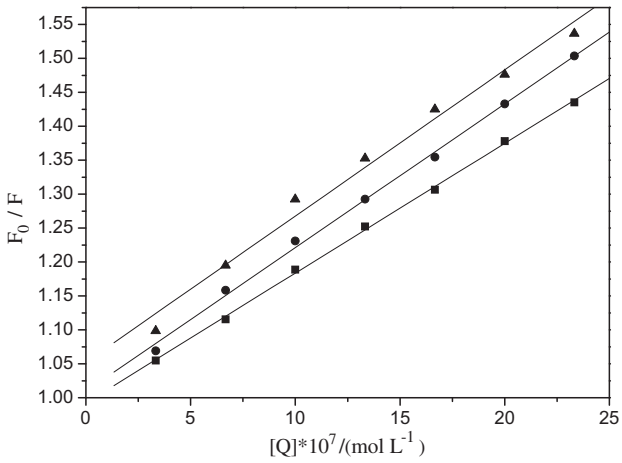

FIGURE 4. The Stern–Volmer plots for the (tanshinone IIA + HSA) system at pH 7.40. HSA concentration: $6.0 \cdot 10^{-3}$ mol · dm^{-3}; (■) T = 296 K; (•) 303 K; (▲) 310 K; λ_{ex} = 280 nm, λ_{em} = 335 nm.

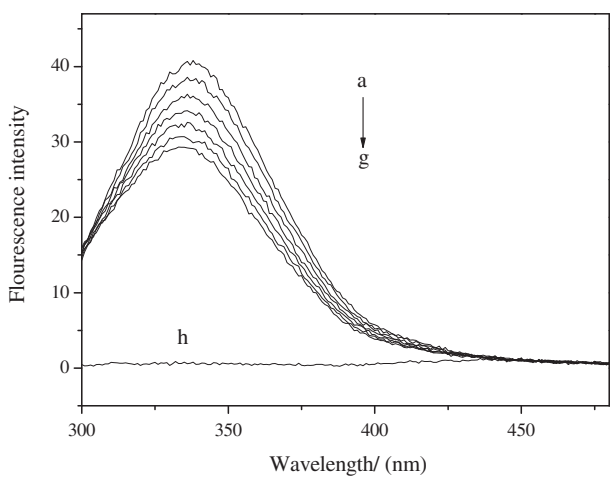

FIGURE 3. The fluorescence emission spectra for the (tanshinone IIA + HSA) system at excited 280 nm: (a) $6.0 \cdot 10^{-6}$ mol · dm^{-3} HSA; (b–g) $6.0 \cdot 10^{-6}$ mol · dm^{-3} HSA in the presence of (0.33, 0.67, 1.00, 1.33, 1.66, and $2.00 \cdot 10^{-6}$) mol · dm^{-3} tanshinone IIA, respectively; (h) $0.67 \cdot 10^{-6}$ mol · dm^{-3} tanshinone IIA. T = 296 K; pH 7.4.

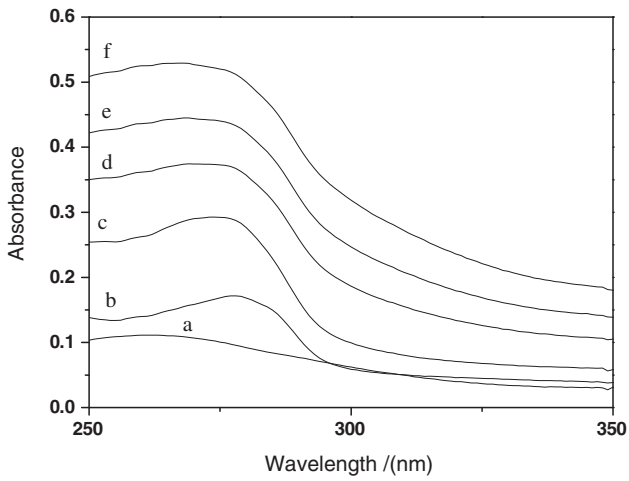

FIGURE 5. UV absorption spectra obtained in Tris buffer solution (pH 7.4): (a) tanshinone IIA, $6.0 \cdot 10^{-6}$ mol · dm^{-3}; (b) HSA, $3.0 \cdot 10^{-6}$ mol · dm^{-3}; (c–f) (tanshinone IIA + HSA), $3.0 \cdot 10^{-6}$ mol · dm^{-3} HSA in the presence of (6.0, 12.0, 18.0, and $24.0 \cdot 10^{-6}$) mol · dm^{-3} tanshinone IIA.

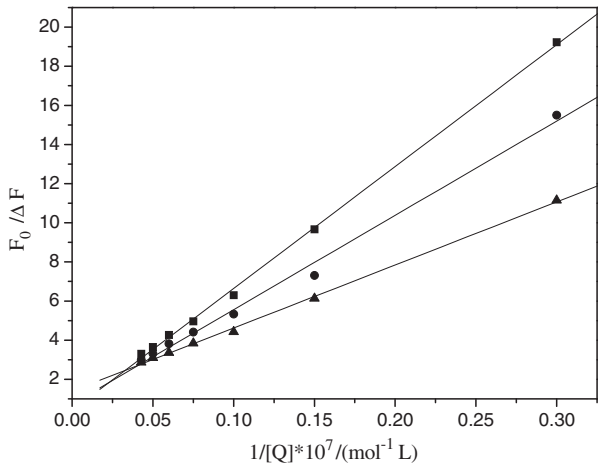

FIGURE 6. Plot of $F_0/\Delta F$ against 1/[Q]: (■) T = 296 K; (●) 303 K; (▲) 310 K; λ_{ex} = 280 nm, λ_{em} = 335 nm, pH 7.4.

TABLE 1
Binding parameters and thermodynamic parameters of (tanshinone IIA + HSA).[a]

T/K	K/ ($dm^3 \cdot mol^{-1}$)	$\Delta G°$/ ($kJ \cdot mol^{-1}$)	$\Delta S°$/ ($J \cdot K^{-1} \cdot mol^{-1}$)	$\Delta H°$/ ($kJ \cdot mol^{-1}$)
296	$6.42 \cdot 10^4$	−27.11	448.12	105.5
303	$1.54 \cdot 10^5$	−30.24	448.12	105.5
310	$4.35 \cdot 10^5$	−33.38	448.12	105.5

[a] T is the temperature at which the experiment was performed; K values were determined from the fluorescence quenching data which were fit using Origin 7 software. The values of $\Delta G°$, $\Delta S°$, and $\Delta H°$ were determined using the equations: $\ln K = -\Delta H°/RT + \Delta S°/R$ and $\Delta G° = \Delta H° - T\Delta S°$; R is the gas constant.

indicated that the static quenching exists in the binding process. In a word, the quenching mechanism of them should be a combined quenching process (including dynamic and static quenching) [27,28].

The fluorescence quenching data were analysed according to the modified Stern–Volmer equation [29]:

$$F_0/\Delta F = 1/(fK_a[Q]) + 1/f. \quad (2)$$

In the present case, F_0 and ΔF are the relative fluorescence intensity without quencher and the difference in fluorescence intensity of protein in the absence and presence of quencher, respectively. The K_a is the binding constant and f is also a constant here, [Q] is the quencher concentration. The plot of $F_0/\Delta F$ against 1/[Q] is linear with the slope equal to the value of $(fK_a)^{-1}$, and the value $1/f$ is fixed on the ordinate. So K_a is a quotient of an ordinate $1/f$ and slope $(fK_a)^{-1}$. Figure 6 shows the linearity in the plot $F_0/\Delta F$ against 1/[Q] at three temperatures (296, 303, and 310) K. The binding constants are listed in table 1 and used to calculate the thermodynamics parameters.

3.3. Determination of binding mode

The binding forces contributing to protein interactions with small molecular substrates may be a van der Waals interaction, an hydrophobic force, or electrostatic interaction, or hydrogen bond [30]. The thermodynamic parameters, enthalpy change ($\Delta H°$), entropy change ($\Delta S°$) and Gibbs free energy change ($\Delta G°$) of reaction are the main evidence for confirming the binding mode. The thermodynamic parameters are evaluated using the following equations:

$$\ln K = -\Delta H°/RT + \Delta S°/R, \quad (3)$$

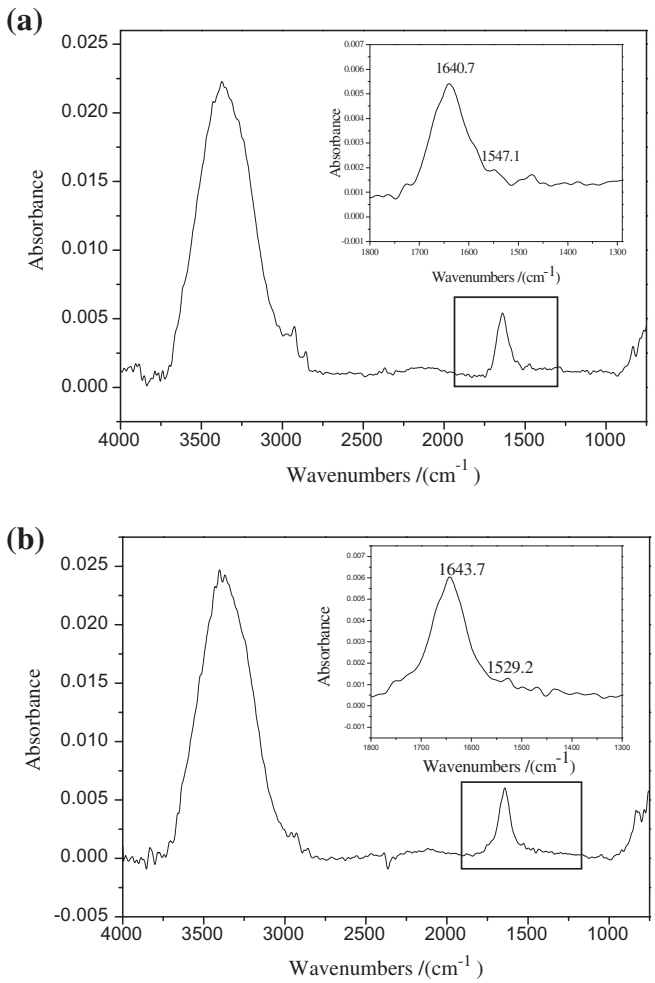

FIGURE 7. FT-IR spectra and difference spectra of HSA. (a) The FT-IR spectra of free HSA (subtracting the absorption of the buffer solution from the spectrum of the protein solution); (b) the FT-IR difference spectra of HSA (subtracting the absorption of the tanshinone IIA-free form from that of (tanshinone IIA + HSA) bound form). Tris–HCl buffer solution, pH 7.40 ($3.0 \cdot 10^{-6}$ mol · dm^{-3}HSA; $6.0 \cdot 10^{-6}$ mol · dm^{-3} tanshinone IIA).

$$\Delta G° = \Delta H° - T\Delta S°, \quad (4)$$

where K and R are the binding constant and gas constant, respectively. The temperature-dependence of the binding constant was studied at three different temperatures (296, 303, and 310) K. By plotting the binding constants, according to Van't Hoff equation, the thermodynamic parameters were determined from the linear Van't Hoff plot (spectrum not shown) and are presented in table 1. As shown in table 1, the values of standard entropy changes ($\Delta S°$) and standard enthalpy changes ($\Delta H°$) of the binding reaction between tanshinone IIA and HSA are found to be both positive. The binding process is endothermic and spontaneous as evidence by the positive $\Delta H°$ and negative of $\Delta G°$. For typical hydrophobic interactions, both $\Delta H°$ and $\Delta S°$ are positive, while negative enthalpy and entropy changes arise from van der Waals force and hydrogen formation in low dielectric media [31]. Therefore, tanshinone IIA bound to HSA was mainly based on hydrophobic interaction, which is in good agreement with the information coming from molecular modelling.

3.4. Changes of the HSA secondary structure induced by tanshinone IIA binding

When drugs bind to protein, the intramolecular forces responsible for maintaining the secondary and tertiary structures can be

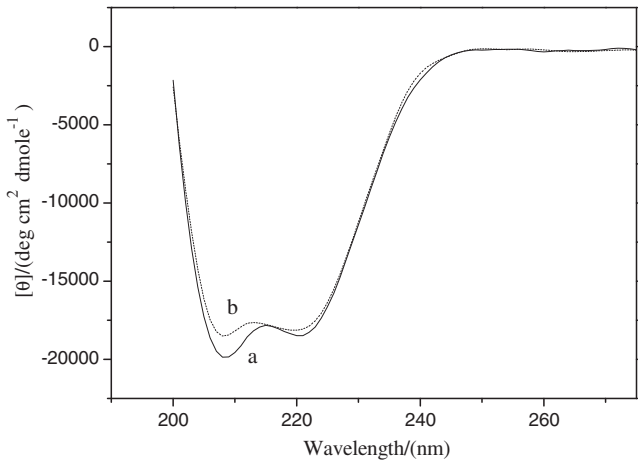

FIGURE 8. CD spectra of HSA and (tanshinone IIA + HSA) system. (a) $3.0 \cdot 10^{-6}$ mol · dm^{-3} HSA; (b) ($3.0 \cdot 10^{-6}$ mol · dm^{-3} HSA + $6.0 \cdot 10^{-6}$ mol · dm^{-3} tanshinone IIA). T = 296 K, pH 7.40.

influenced, leading to a conformational change of the protein [32]. In addition, the conformational change of the protein can be reflected in the infrared absorption spectra or CD spectra.

The FT-IR spectroscopy was investigated to obtain more information on the binding of tanshinone IIA to HSA. Infrared spectra of proteins exhibit a number of the so-called amide bands, which represent different vibrations of the peptide moiety. Of all the amide bands of the protein, amide I ranging from (1600 to 1700) cm^{-1} (mainly C=O) and amide II ≈ 1548 cm^{-1} (mainly C–N) have been widely used as typical ones [33,34]. They both have a relationship with the secondary structure of the protein. Figure 7 is the FT-IR spectra of the HSA and tanshinone IIA-bound form of HSA with its difference absorption spectrum. It can be seen in figure 7 that the peak positions of amide I band (1640.7 cm^{-1}) and amide II band (1547.1 cm^{-1}) have obvious shifts and their peak shapes are also changed. So we conclude that the addition of tanshinone IIA has changed the secondary structure of HSA.

To ascertain the possible influence of tanshinone IIA binding on the secondary structure of HSA, CD studies were performed in the presence of tanshinone IIA. Figure 8 shows the CD spectra of HSA and (tanshinone IIA + HSA) complex. The CD spectra of HSA exhibit two negative bands in the ultraviolet region at (208 and 218) nm, which is characteristic of the α-helical structure of protein. The reasonable explanation is that the negative peaks between (208 to 209 and 222 to 223) nm both contribute to the n–π* transfer for the peptide bond of the α-helical structure [35]. From figure 8, it can be seen that the addition of tanshinone IIA leads to the change of the spectra in the position and the intensity of the bands. The calculated results exhibit a reduction of the α-helical structure from 54.68% to 50.02% at a mole ratio tanshinone IIA/HSA of 2:1. The result reveals that the binding of tanshinone IIA to HSA has changed the secondary structure of HSA.

4. Conclusions

The interactions between tanshinone IIA and HSA have been investigated using molecular modelling and different optical techniques. The molecular modelling study provides the theoretical direction before experiments in order to get more reliable experimental results. The results obtained from molecular modelling indicate that the interaction between tanshinone IIA and HSA is dominated by the hydrophobic force. The experimental results suggest that tanshinone IIA could bind tightly to HSA. The binding process is endothermic and spontaneous as evidences by the positive ΔH° and negative of ΔG°. In addition, CD and FT-IR spectroscopy showed that the secondary structure of HSA is changed after tanshinone IIA bound to HSA.

Acknowledgements

This work was financially supported by the National Natural Science Foundation of China (Grant No. 21103133).

References

[1] B.L. Zhao, W. Jiang, Y. Zhao, J.W. Hou, W.J. Xin, Biochem. Mol. Biol. Int. 38 (1996) 1171–1182.
[2] S.L. Yuan, X.J. Wang, Y.Q. Wei, Ai. Zheng. 22 (2003) 1363–1366.
[3] X.J. Wang, Y.Q. Wei, S.L. Yuan, G.J. Liu, Y.R. Lu, J. Zhang, W.D. Wang, Int. J. Cancer. 116 (2005) 799–807.
[4] E.H. Cao, X.Q. Liu, J.J. Wang, N.F. Xu, Free Radic. Biol. Med. 20 (1996) 801–806.
[5] Y.F. Ueng, Y.H. Kuo, S.Y. Wang, Y.L. Lin, C.F. Chen, Life Sci. 74 (2004) 885–896.
[6] A. Robertson, R. Brodersen, Dev. Pharmacol. Ther. 17 (1991) 95–99.
[7] H. Vorum, B. Honore, J. Pharm. Pharmacol. 48 (1996) 870–875.
[8] W.Y. He, Y. Li, C.X. Xue, Z.D. Hu, X.G. Chen, F.L. Sheng, Bioorg. Med. Chem. 13 (2005) 1837–1845.
[9] Y. Li, W.Y. He, J.Q. Liu, F.L. Sheng, Z.D. Hu, X.G. Chen, Biochim. Biophys. Acta 1722 (2005) 15–21.
[10] A. Barik, B. Mishra, A. Kunwar, K.I. Priyadarsini, Chem. Phys. Lett. 436 (2007) 239–243.
[11] J.N. Tian, J.Q. Liu, J.Y. Zhang, Z.D. Hu, X.G. Chen, Chem. Pharm. Bull. 51 (2003) 579–582.
[12] M. Jiang, M.X. Xie, D. Zheng, Y. Liu, X.Y. Li, X. Chen, J. Mol. Struct. 692 (2004) 71–80.
[13] J.H. Li, C.L. Ren, Y.H. Zhang, X.Y. Liu, X.J. Yao, Z.D. Hu, J. Mol. Struct. 881 (2008) 90–96.
[14] I. Petitpas, A.A. Bhattacharya, S. Twine, M. East, S. Curry, J. Biol. Chem. 276 (2001) 22804–22809.
[15] G. Morris, SYBYL Software, Version 6.9, St. Louis, Tripos Associates Inc., 2002.
[16] A. Dong, P. Huang, W.S. Caughey, Biochemistry 29 (1990) 3303–3308.
[17] J.Q. Liu, J.M. Tian, X. Tian, Z.D. Hu, X.G. Chen, Bioorg. Med. Chem. 12 (2004) 469–474.
[18] Z.X. Lu, T. Cui, Q.L. Shi, Applications of Circular Dichroism (CD) and Optical Rotatory Dispersion (ORD) Molecular Biology, first ed., Science Press, Beijing, 1987.
[19] I. Sjoholm, B. Ekman, A. Kober, I. Ljungstedt-Pahlman, B. Seiving, T. Sjodin, Mol. Pharmacol. 16 (1979) 767–777.
[20] X.M. He, D.C. Carter, Nature 358 (1992) 209–215.
[21] D.C. Carter, X.M. He, S.H. Munson, P.D. Twigg, K.M. Gernert, M.B. Broom, T.Y. Miller, Science 244 (1989) 1195–1196.
[22] J.R. Lakowicz, Principles of Fluorescence Spectroscopy, second ed., Kluwer Academic Publishers/Plenum Press, New York, 1999. pp. 237–259.
[23] T.S. Singh, S. Mitra, Spectrochim. Acta A 78 (2011) 942–948.
[24] M. Xu, Z.R. Ma, L. Huang, F.J. Chen, Z.Z. Zeng, Spectrochim. Acta A 78 (2011) 503–511.
[25] S. Ashoka, J. Seetharamappa, P.B. Kandagal, S.M.T. Shaikh, J. Lumin. 121 (2006) 179–186.
[26] Y.J. Hu, Y. Liu, J.B. Wang, X.H. Xiao, S. Qu, J. Pharm. Biomed. Anal. 36 (2004) 915–919.
[27] H.W. Zhao, M. Ge, Z.X. Zhang, W.F. Wang, G.Z. Wu, Spectrochim. Acta A 65 (2006) 811–817.
[28] J. Zhang, D.X. Xiong, L.G. Chen, Q.L. Kang, B.R. Zeng, Spectrochim. Acta A 96 (2012) 132–138.
[29] S. Lehrer, Biochemistry 10 (1971) 3250–3254.
[30] C.Q. Jiang, M.X. Gao, X.Z. Meng, Spectrochim. Acta A 59 (2003) 1605–1610.
[31] J.N. Tian, J.Q. Liu, J.P. Xie, X.J. Yao, Z.D. Hu, X.G. Chen, J. Photochem. Photobiol. B 74 (2004) 39–45.
[32] U. Kragh-Hansen, Pharmacol. Rev. 33 (1981) 17–53.
[33] V.A. Sirotkin, A.N. Zinatullin, B.N. Solomonov, D.A. Faizullin, V.D. Fedotov, Biochim. Biophys. Acta 1547 (2001) 359–369.
[34] Q.Q. Bian, J.Q. Liu, J.N. Tian, Z.D. Hu, Int. J. Biol. Macromol. 34 (2004) 275–279.
[35] P. Yang, F. Gao, The Principle of Bioinorganic Chemical, Science Press, 2002. p. 349.